Published by Elsevier Inc.

ISSN 0735-1097/03/$30.00
doi:10.1016/S0735-1097(03)00828-3

BASIC RESEARCH

Dendritic Cells in Neointima Formation After Rat Carotid Balloon Injury: Coordinated Expression With Anti-Apoptotic Bcl-2 and HSP47 in Arterial Repair

Gerhard Bauriedel, MD, FACC,* Alexander Jabs, BS,* Dirk Skowasch, MD,* Randolph Hutter, MD,† Juan J. Badimon, PHD, FACC,† Valentin Fuster, MD, PHD, FACC,† Ulrich Welsch, MD, PHD,‡ Berndt Lüderitz, MD, FACC*

Bonn and Munich, Germany; and New York, New York

OBJECTIVES We sought to evaluate: 1) the contribution of dendritic cells (DCs); and 2) the impact of B-cell lymphoma 2 protein (Bcl-2), a central anti-apoptotic protooncogene, and of heat shock protein 47 (HSP47), indicating subsequent collagen deposition, in neointima formation after angioplasty.

BACKGROUND The origin of neointimal cells and the factors that promote their accumulation are still unclear. Previous studies reported intimal presence of DCs and suggested cells of primarily extravascular origin to contribute to arterial repair.

METHODS Sprague-Dawley rats underwent carotid balloon angioplasty. At different times after angioplasty, tissue sections were analyzed by immunohistochemistry using OX-62 and S100 as DC markers and antibodies against Bcl-2 and HSP47, supplemented by electron microscopic analysis of cell type and apoptosis.

RESULTS Four days after injury, DCs adhered along the internal elastic lamina and demonstrated intense Bcl-2 and HSP47 expression, consistent with low apoptosis. With ongoing neointima enlargement, luminal DCs remained prevalent and were colocalized with Bcl-2 and HSP47, while signaling decreased to basal regions. Media showed no DCs and only low Bcl-2 and HSP47 immunoreactivity. Adventitia transiently revealed a structural separation between day 4 and 7. Whereas the inner layer demonstrated sparse cellularity, apoptosis and no DC, Bcl-2, and HSP47 labeling, the outer layer was characterized by high myofibroblast density with strong Bcl-2 and HSP47 expression but absence of DCs.

CONCLUSIONS We identify DCs as novel components in early neointima formation, promoted by coordinated anti-apoptotic Bcl-2 and HSP47 expression. Despite intense adventitial remodeling, there is no evidence of adventitial cell transmigration. (J Am Coll Cardiol 2003;42: 930–8) © 2003 by the American College of Cardiology Foundation

To abrogate restenosis and in-stent restenosis, future generations of drug-eluting stents may profit from a better understanding of the pathogenic determinants leading to intimal hyperplasia. Indeed, there is still a paucity of data on: 1) the origin of neointimal cells; 2) the determinants that allow these cells to survive in their environment; and 3) the early events that contribute to neointima formation.

See page 939

Traditional concepts in vascular repair comprise proliferation, migration, and differentiation of smooth muscle cells (SMCs) and other cells (1–4). Of note, recent work has focused attention on circulating bone marrow-derived progenitor cells as a source of neointimal cells that contribute to restenosis, graft vasculopathy, and hyperlipidemia-induced atherosclerosis, possibly differentiating to SMCs (5,6). Likewise, bone marrow-derived endothelial and SMC progenitor cells that share the surface marker CD34 were found involved in arterial remodeling and neovascularization (7–10).

Most interestingly, dendritic cells (DCs) have also been generated from myeloid $CD34^+$ progenitors (11,12), pointing to a common bone marrow origin with other blood-borne precursors. So far, four stages of DC development have been delineated: 1) bone marrow progenitors; 2) circulating DC precursor cells; 3) tissue-residing immature DCs; and 4) mature DCs as the most potent antigen-presenting cells that prime "naive" T cells and initiate specific immune responses (11). As to vascular pathology, DCs were found in atherosclerotic plaques, apparently involved in local immune-inflammatory reactions (13–15). Also, a subendothelial network of DCs considered to be part of the vascular-associated lymphoid tissue was detected in the arteries of healthy young individuals at sites predisposed for late lesion formation (16,17). Vascular DCs in arterial specimens were identified by S100, an intracellular calcium-binding protein, and by typical ultrastructural fea-

From the *Department of Medicine–Cardiology, University of Bonn, Bonn, Germany; †The Zena and Michael A. Wiener Cardiovascular Institute, Mount Sinai School of Medicine, New York, New York; and the ‡Institute of Anatomy, University of Munich, Munich, Germany. Supported, in part, by the BMBF (German Bundesministerium für Bildung und Forschung, Bonn, Germany) grant 01KV9915 (to G.B.).

Manuscript received June 27, 2002; revised manuscript received April 9, 2003, accepted April 24, 2003.

Abbreviations and Acronyms

Bcl-2 = B-cell lymphoma 2 protein
CD34 = hematopoietic stem cell marker
DC = dendritic cell
EC = endothelial cell
HSP47 = heat shock protein 47
OX-62 = dendritic cell marker
S100 = dendritic cell marker
SMC = smooth muscle cell
TEM = transmission electron microscopy

tures (14,15). Likewise in rats, the monoclonal OX-62 antibody that immuno-precipitates a molecule with α-integrin–like properties allowed for immunolabeling of bone marrow-derived DCs (18).

Given the demand for a rapid controlled repair at the injured vascular site, implicated cells should be protected to survive in their local environment. Accordingly, recent reports stressed the importance of a delicate balance between pro- and anti-apoptotic mediators of the B-cell lymphoma 2 protein (Bcl-2) family for progression and regression of vascular disease (19–21). The Bcl-2 protooncogene encodes an intracellular membrane-associated protein that acts as an inhibitor of apoptosis in various cell types including hematopoietic stem cells (22), DCs (23), and vascular SMCs (19). Heat shock protein 47 (HSP47), indicating subsequent collagen deposition essential for cell anchorage and survival, is a 47 kDa intracellular glycoprotein from the serpin superfamily. Heat shock protein 47 transiently binds to newly synthesized procollagen and dissociates from procollagen during its transport from the endoplasmic reticulum to the cis-Golgi compartment (24). Interestingly, HSP47 knockout mice displayed ruptured blood vessels and abnormally orientated epithelium (24), and HSP47 was found expressed in human fibrous atheroma (25) and was low in coronary atherectomy specimens with acute coronary syndromes compared with stable angina (26).

In the present series of experiments, we examined the presence of neointimal DCs and the coordinated expression of Bcl-2 and HSP47 as two important determinants for cell survival and matrix formation after balloon angioplasty of rat carotid arteries compared with non-injured controls. These studies identified DCs as novel cellular components involved in early neointima formation, while not supporting transmigration of adventitial cells and, thereby, suggesting circulating blood and/or the intima as the source of neointimal cells.

METHODS

Rat carotid angioplasty. Male Sprague-Dawley rats (350 to 400 g) were anesthesized with an intraperitoneal injection of ketamine (100 mg/kg, Parke-Davis Inc., Berlin, Germany) and xylazine (15 mg/kg, Bayer Inc., Leverkusen, Germany). Balloon angioplasty of the common carotid artery was performed using a Fogarty 2F balloon embolectomy catheter (Baxter Inc., Munich, Germany) as previously described (1,3). The right carotid artery was surgically exposed but not injured. At 0, 4, 24, and 48 h, 4, 7, 14, and 28 days after injury, 6 rats/time point were euthanized, and both carotid arteries were excised. Animal investigation was conform to the "Position of the American Heart Association on Research Animal Use" adopted by the American Heart Association November 11, 1984. Animal studies were approved by the Committee for the Care and Use of Animals of the Government of Oberbayern, Germany (AZ 211-2531).

Arteries were divided into two segments of equal size and without additional manipulations, fixed in buffered 4% formaldehyde for immunohistochemistry or in 3.5% glutaraldehyde for transmission electron microscopy (TEM). Of note, the technique by which the artery was excised and tissue preparation with avoidance of transluminal fixative perfusion was regarded to be important in order to preserve the innermost vascular wall layer.

Immunohistochemistry. Immunohistochemistry was performed in 4 μm paraffin-embedded arterial cross sections after proteolysis with either 3% citrate (pH 6.0) or target unmasking fluid (PanPath Inc., Amsterdam, the Netherlands). Non-specific antibody binding sites were blocked by fetal calf serum at a dilution of 1:25 for OX-62, S100, CD31, and HSP47, or by rabbit serum 1:20 for Bcl-2. Sections were then treated with either the monoclonal mouse anti-rat dendritic cell (1:20, Pharmingen Inc., Heidelberg, Germany, clone OX-62), mouse anti-rat CD31 (1:100, Biozol Inc., Eching, Germany, clone TLD-3A12), or mouse anti-rat HSP47 antibodies (1:1,000, Calbiochem Inc., Heidelberg, Germany, clone M16.10A1), or the polyclonal rabbit anti-S100 (1:100, Sigma Inc., Munich, Germany, catalog number S2644), or rabbit anti-rat Bcl-2 antibodies (1:50, Pharmingen Inc., catalog number 13456E) for 12 h at 4°C. Selected sections were incubated with monoclonal antibodies to α-SM actin (1:75, Boehringer Inc., Mannheim, Germany, clone asm-1) or stained by Masson Goldner trichrome. For polyclonal antibodies, AffiniPure mouse anti-rabbit IgG (1:75, Dianova Inc., Hamburg, Germany, code-number 211-005-109) was applied for 30 min at room temperature after primary antibody incubation. Primary antibodies bound to their target protein were visualized with the APAAP technique (Boehringer) and Fast Red (Sigma), and nuclei were counterstained with hematoxylin.

Double staining experiments were performed with OX-62/S100, OX-62/Bcl-2, and OX-62/HSP47. After OX-62 immunostaining with the APAAP method as described above and Fast Blue (Sigma) as chromogen, tissue sections were washed in phosphate-buffered saline (pH 7.3). Consecutively, sections were incubated with either S100, Bcl-2, or HSP47 antibodies for 12 h at 4°C. For polyclonal S100 and Bcl-2, AffiniPure mouse anti-rabbit IgG was subsequently applied as described above. Bound S100, Bcl-2, or HSP47 antibodies were visualized by APAAP and Fast

Red. To improve the detection of Fast Blue immunostaining, hemotoxylin nuclear staining was omitted. To determine the OX-62 antibody specificity, rat spleen tissue sections known to contain large amounts of DCs were taken as positive controls. Additional positive controls used were rat spleen and rat para-aortic lymph nodes for S100, non-traumatized rat carotid arteries for CD31, rat thymus for Bcl-2 and HSP47, and rat aortic segments for α-SM actin (not shown). Tissue sections without primary antibody incubation served as negative controls in each staining procedure, according to previous reports (14,15,17). To exclude non-specific immunostaining, rat myocardial sections were used as negative controls and showed no immunoreactivity.

Histologic analysis. A computer-assisted morphometric system (VFG-1-grafic card/VIBAM 0.0 Software) was used to automatically count labeled nuclei per defined area (20,27). Area, cellularity, and the percentage of OX-62-, S100-, Bcl-2-, and HSP47-labeled cells were evaluated for neointima, media, and adventitial layers from six randomly selected fields per cross-section. The percentage of labeled cells was expressed as the number of positive cells per total number of cells for each layer (20).

Transmission electron microscopy. Transmission electron microscopy analysis of tissue segments was performed according to standard protocols (20,27). Non-overlapping images of randomly selected compartment regions were photographically enlarged to a final magnification of $\times$8,300. For each traumatized arterial segment, a total of 20 photographs (17 $\times$ 21 cm each) were taken, and 6 to 12 vascular cells were classified as SMCs, DCs, macrophages, or lymphocytes. All together, recognition of >1,200 vascular cells was performed according to ultrastructural features. Dendritic cells were identified by the presence of numerous long dendritic processes and veils, lobed nuclei, profuse mitochondria, and a prominent tubulovesicular system (14,15). Smooth muscle cells, macrophages, and lymphocytes were classified according to ultrastructural features, as previously reported in detail (27–30). The identification of apoptotic cells was based upon specific morphological criteria as defined in several reports (20,27,28).

Statistical analysis. All values are expressed as mean $\pm$ SEM. Statistical significance was evaluated with a two-tailed unpaired Student t test for comparisons between the means of two groups. Two-tailed bivariate correlations were determined by the Pearson coefficient. The SPSS for Windows software (version 10.0.7, SPSS Inc., Chicago, Illinois) was used for statistic analysis. A value of $p < 0.05$ was interpreted to denote statistical significance.

RESULTS

Rat carotid arteries were analyzed 0, 4, 24, and 48 h, 4, 7, 14, and 28 days after balloon angioplasty. Transmural response in regard to compartment area, cellularity, expression of OX-62, S100, Bcl-2, and HSP47, apoptosis, and cell type was compared to non-injured arteries. Spatiotemporal increase in neointimal and adventitial area as well as in cellularity (Fig. 1) demonstrated the adequacy of the injury model used to study specific mechanisms underlying neointima formation and concomitant transmural remodeling.

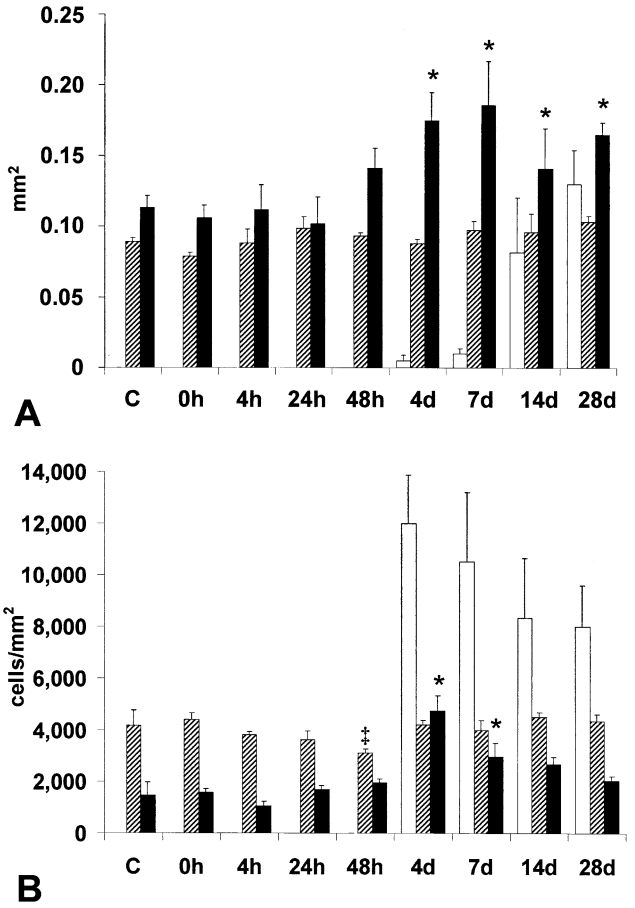

Figure 1. Bar graph demonstrating mean area **(A)** and cellularity **(B)** of each vascular compartment during time course. **Open bars** = neointima; **hatched bars** = media; **solid bars** = adventitia. *$p < 0.05$ vs. baseline, as indicated. Of note, medial cellularity decreased by 29% (‡$p = 0.002$) at 48 h compared with baseline and recovered ($p = 0.001$) at day 4 (not marked). Uninjured control segments (C) did not show neointima formation or altered structure of media and adventitia.

Neointima. As early as day 4 after injury, single cells adhered along the internal elastic lamina in a palisade-like arrangement (Fig. 2A). A significant proportion of early neointimal cells was identified as DCs due to strong cell-bound OX-62 labeling (Fig. 2B), S100 immunostaining (Fig. 2C), and characteristic ultrastructural features (Fig. 2D). In addition, TEM analysis proved low apoptosis in the neointima at days 4 and 7 with 2% and 5%, respectively (Fig. 2E). Gradually, intimal cells accumulated to circumferential uniform layers (Figs. 2F to 2H) expanding to a neointimal territory with high cellularity (Fig. 1). At seven days after injury, immunoreaction for DCs was maximal (45 $\pm$ 14%), and significantly decreased at later time points (Fig. 3A). Rat spleen sections taken as positive controls consistently demonstrated intense OX-62

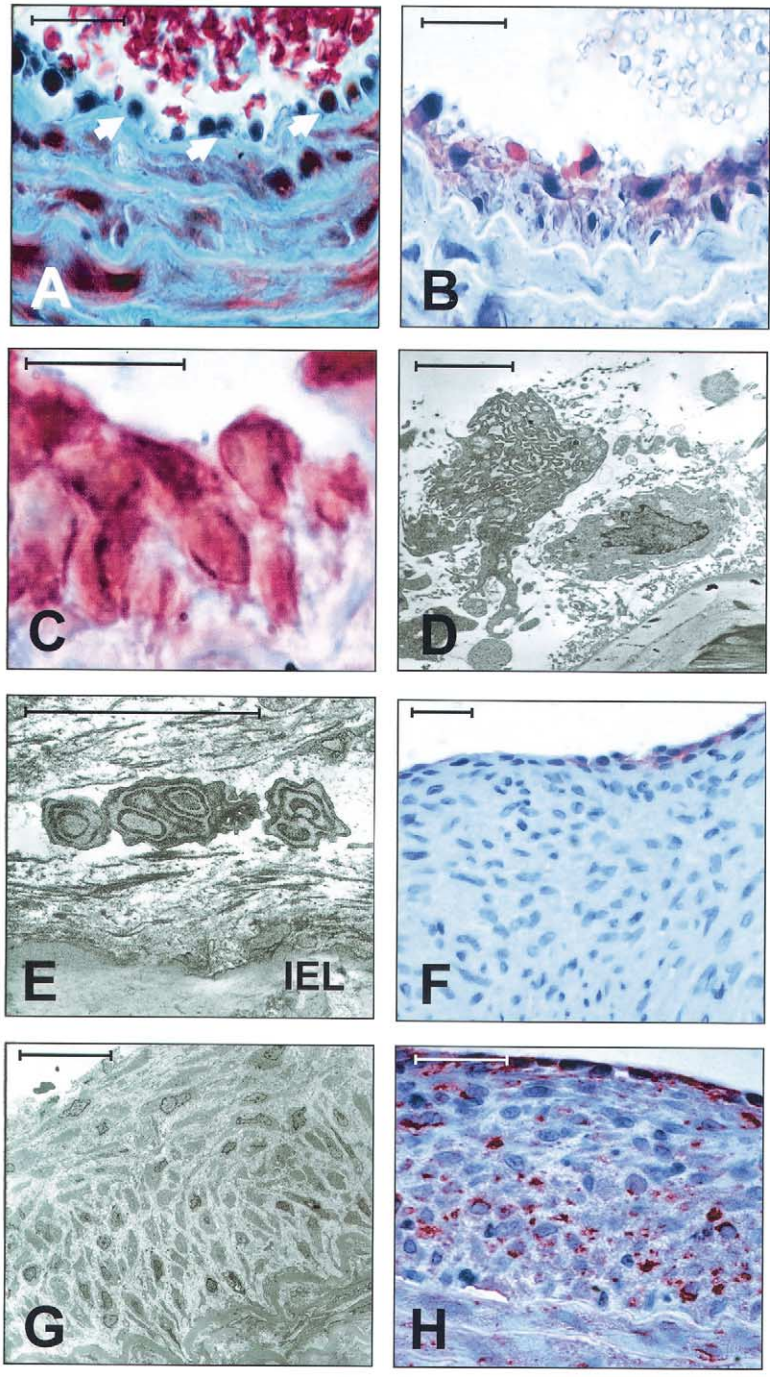

Figure 2. Photomicrographs of early neointima formation, focused on the luminal surface region. **(A)** Palisade-like alignment of single cells **(arrows)** along the internal elastic lamina (IEL) at day 4 (trichrome staining). **(B)** Strong cell-bound OX-62 signaling restricted to early neointima contrasts to unlabeled media at day 7. **(C)** Magnified detail of neointima at day 7 demonstrating consistent colocalization of OX-62 **(dark blue)** and S100 **(red)** in neointimal dendritic cells (DC) (no nuclear counterstaining). **(D)** Transmission electron microscopy identification of two DCs extending along the IEL at day 7. Note their long dendritic processes and veils, the lobed nucleus, and prominent tubulovesicular network. **(E)** Transmission electron microscopy detection of apoptosis located in basal neointima close to IEL. Apoptotic shrinkage and detached anchorage from surrounding extracellular matrix are indicated by condensed cytoplasm and pericellular region markedly less dense than adjacent matrix. **(F)** Representative hyperplastic neointima at day 28. Note the distinct residual OX-62 labeling along the luminal surface, while the vast majority of cells located in basal regions are negative. **(G)** Transmission electron microscopy image of representative hyperplastic neointima at day 28 that predominantly comprises cells with SMC appearance and apparently shows no apoptosis. Luminal neointima reveals perpendicular alignment of the cells and loose extracellular matrix compared with basal regions. **(H)** Intense α-smooth muscle actin immunoreactivity of the neointima and weak staining of medial SMCs at day 28. **Bar** = 30 μm **(A to C, F to H)**; **bar** = 5 μm **(D, E)**.

immunoreactivity (Fig. 3B). Neither endothelial cells nor macrophages and only a few lymphocytes (<2%) were detected in the neointima at this time and later, when most of the neointimal cells were positive of α-smooth muscle actin (Figs. 2G and 2H). In 28-day injured arteries, DCs were found exclusively at the luminal surface, while most of

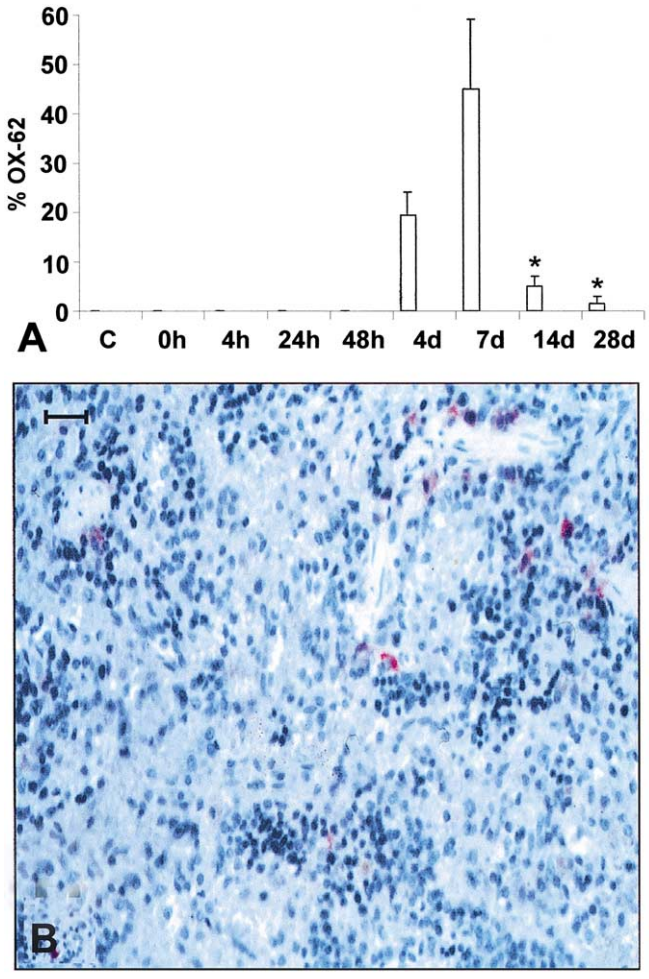

Figure 3. Dendritic cells in early neointima formation. **(A)** Bar graph demonstrating percentage of neointimal OX-62$^+$ dendritic cells (DC) after angioplasty. **Open bars** = neointima. $^*p < 0.05$ versus value at seven days. **(B)** Staining of DCs in rat spleen as positive control for OX-62. **Bar** = 30 μm **(B)**.

the structured neointima contained cells with SMC appearance, and apoptosis was <1% (Fig. 2G).

Neointimal cells showed strongly cell-bound signals of the anti-apoptotic Bcl-2 protooncogene by day 4 (Fig. 4A). Later, at days 14 and 28, Bcl-2-stained cells were predominantly localized close to the luminal surface, and gradually decreased to basal neointima (Figs. 4B and 4C). Double immunostaining demonstrated OX-62$^+$ DCs to have high Bcl-2 expression (Fig. 4C). Quantified expression of Bcl-2 in neointima with time is outlined in Figure 5A. In serial sections HSP47, indicating subsequent collagen deposition, demonstrated a similar postangioplasty expression pattern as Bcl-2 (Figs. 4D to 4F, and 5B). There was coexpression of OX-62 and HSP47 at the luminal surface that disappeared to deeper neointimal areas (Fig. 4F). Throughout the time course of neointima formation, a positive relationship was seen between the expression of HSP47 and that of Bcl-2 ($r = 0.49$, $p = 0.04$). At day 28 a strong positive correlation between HSP47 expression and neointimal area was found ($r = 0.86$, $p = 0.03$). In contrast, luminal non-traumatized control segments consistently revealed no signals of either OX-62, S100, Bcl-2, or HSP47.

Media. The time course of medial area and cellularity after angioplasty was remarkably constant between 4 and 28 days (Fig. 1). No DCs were detected at any time point. Specific signals of Bcl-2 were first seen at 48 h after angioplasty and were maximal (9%) at day 14 beyond an overall low expression, whereas HSP47 immunoreactivity was constant (5%) within a constitutive expression profile (Fig. 5).

Adventitia. Adventitial remodeling, indicated by a significant increase in compartment area and cellularity, was present as early as days 4 and 7 (Fig. 1). During this period, a transient structural separation of the adventitia occurred resulting in an inner hypocellular and an outer hypercellular layer with strong α-SM actin signaling and intense neovascularization (Fig. 6A). Ultrastructurally, the inner zone contained several apoptotic cells and large areas of non-organized extracellular matrix, while the outer zone comprised numerous viable fibroblast-like cells embedded in structured collagen matrix and several microvessels (Figs. 6B and 6C). Adventitial cells demonstrated no immunoreactivity indicating presence of DCs, whereas neointimal cells displayed intense labeling (Fig. 6D). Adventitial cells located in the outer zone showed strong signaling of both Bcl-2 and HSP47 with maximal expression of 29% and 57%, respectively (Figs. 5, 6E and 6F). At no time point studied were signals of either OX-62, S100, Bcl-2, and HSP47 detected in the inner hypocellular zone of the adventitia.

DISCUSSION

DCs in early neointima formation. As the central finding, our data consistently demonstrate the early apposition of DCs along the injured artery, maximal DC frequency between days 4 and 7, and distinct luminal preservation up to day 28, when expression decreased (Figs. 2 and 3). The presence of DCs in the context with postangioplasty neointima formation is new and intriguing, and adds another facet to previous, traditional, as well as novel concepts concerning the origin and nature of neointimal cells (1–6,31). So far, DCs were detected in human carotid plaques (14) and aortic lesions of hypercholesterolemic rats (15), suggesting local immune-inflammatory reactions. Another report on autopsy arteries from young adults supported a role of vascular DCs as a nidus of subsequent lesion formation (17), and, most recently, activated DCs were shown to contribute to the progression of atherosclerosis (32).

Our findings of OX-62$^+$S100$^+$ DCs and absence of macrophages and endothelial cells (ECs) in incipient neointima as early as day 4 point to a definite time, when homing of DCs begins. It is known that inflammatory cells are present along the luminal surface of the injured artery from 2 h to three days. Among these cells, neutrophils and macrophages express messenger RNAs encoding cell adhe-

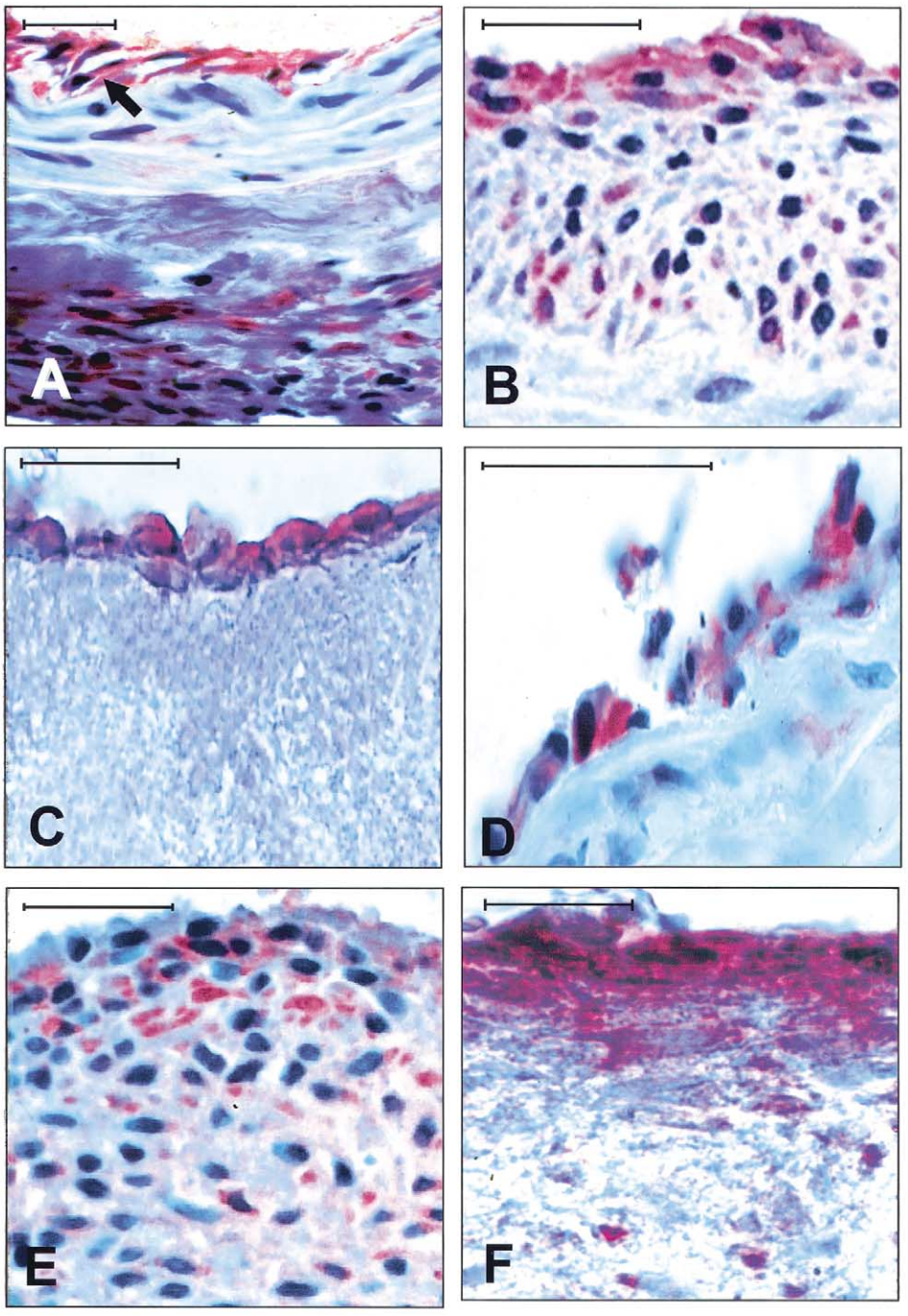

Figure 4. Photomicrographs of specific B-cell lymphoma 2 protein (Bcl-2) **(A to C)** and heat shock protein 47 (HSP47) immuno-staining **(D to F)** in neointima formation from day 4 to day 28 after injury. **(A)** Strongly cell-bound signaling of Bcl-2 in incipient neointima formation at day 4 **(arrow)**. **(B)** Luminal prevalence of Bcl-2-positive cells and declining expression in basal regions at day 14. **(C)** Double staining for OX-62 **(dark blue)** and Bcl-2 **(red)** in neointima at day 28 demonstrating persistent luminal prevalence of Bcl-2^+ dendritic cells (no nuclear counterstaining). **(D)** Luminal cells adhering to the internal elastic lamina exhibit strong HSP47 labeling at day 4. **(E)** Heat shock protein 47 signals are maximal at the luminal surface and continuously decrease to basal regions at day 28. **(F)** Double staining for OX-62 **(dark blue)** and HSP47 **(red)** in neointima at day 14. Note dendritic cell-bound neointimal HSP47 expression at the luminal border and sparse HSP47 immunoreactivity without presence of dendritic cells in deep neointimal areas (no nuclear counterstaining). **Bar** = 30 μm **(A to F)**.

sion molecules and chemokines (33). In consequence, these factors could very well induce recruitment and homing of DCs (11). Our present data show the onset of neointima formation at days 4 and 7, parallel to the profile of DC marker expression that is maximal within the same time window (Fig. 3A), while advanced neointima was predominantly composed of α-smooth muscle actin$^+$ SMCs (Figs. 2G and 2H). Likewise, Sata et al. (5) reported that bone marrow-derived neointimal cells in mice were negative for markers of SMCs and ECs, when they attached to the

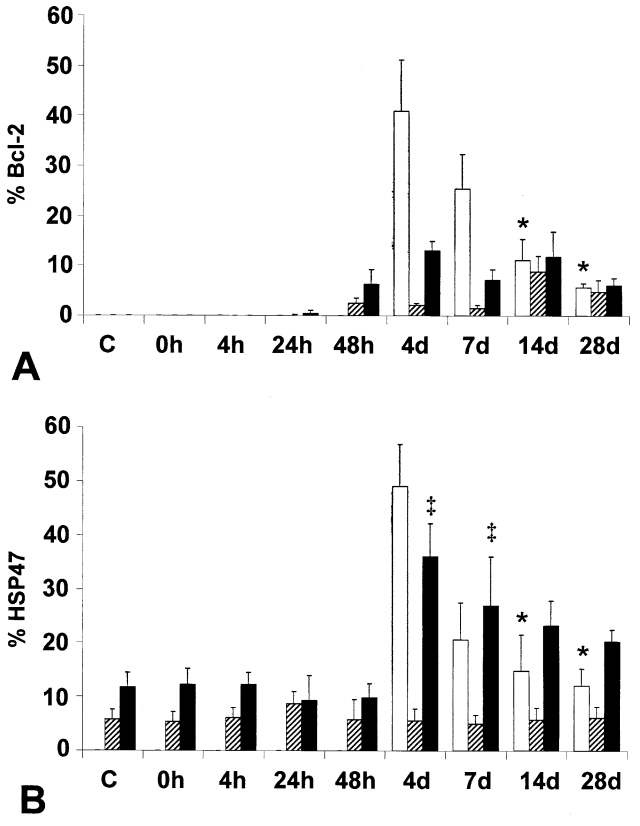

Figure 5. Bar graph demonstrating mean expression of B-cell lymphoma 2 protein (Bcl-2) **(A)** and of heat shock protein 47 (HSP47) **(B)** in each vascular compartment during time course. **Open bars** = neointima; **hatched bars** = media; **solid bars** = adventitia. *$p < 0.05$ versus value at four days, as indicated for neointima; ‡$p < 0.05$ versus baseline, as indicated for adventitia.

luminal site of the artery 7 days after injury. Later, the dilated lumen gradually narrowed due to neointimal hyperplasia primarily composed of SMCs (5). Also, Christen et al. (4) showed percentages of α-smooth muscle actin$^+$ neointimal cells that increased from 26% at day 7 to 98% at day 30 in injured porcine coronary arteries. Disappearance of DC markers and presence of SMC features could mean that a proportion of DCs migrate out of the neointima or that DC apposition decreases with time after injury. Other possibilities may be transdifferentiation into SMCs as recently shown for hematopoietic stem cells (5) or neointimal cell death, although the latter is not supported by our present data that consistently demonstrate low neointimal apoptosis between days 4 and 28.

Coordinated Bcl-2 and HSP47 expression in DCs and neointimal cell accumulation. Parallel to incipient lesion formation, we observed a strong Bcl-2 labeling of neointimal cells. Although expression of Bcl-2 decreased later like those of OX-62 and S100, the luminal prevalence of Bcl-2$^+$ DCs persisted (Figs. 2F, 4B, 4C, and 5A); Bcl-2 is known to mediate DC longevity (23); decreased Bcl-2 expression reduced the viability of CD34$^+$-derived DCs in vitro (34). Also, cultured aortic SMCs were found to be resistant to apoptosis after transfection by a retroviral vector for Bcl-2 (19). Consistent with apoptosis data in a postangioplasty rabbit model (35), our TEM findings demonstrate neointimal apoptosis as low as 2% and 5% at days 4 and 7, which is the peak of Bcl-2 expression. A low 3% level of apoptosis was also found in hyperplastic human restenosis (20). Taken together, our present data support the concept of an upregulated anti-apoptotic Bcl-2 expression of luminally adherent DCs and adjacent cells in basal neointima to preserve cellular integrity until neointimal tissue consolidation occurs.

Heat shock protein 47 was expressed in neointima remarkably similar to the expression profile of Bcl-2 and was clearly colocalized with DC markers in luminally adherent cells (Figs. 4F and 5B). Heat shock protein 47 triggers collagen synthesis and matrix deposition that allow cellular anchorage and antagonize a special form of apoptosis called anoikis (36), thereby again supporting neointimal cells to survive. Indeed, in view of low apoptosis, the present study shows positive relationships between Bcl-2 and HSP47 and between HSP47 and neointimal area at day 28. These findings may strengthen the concept of coordinated anti-apoptotic signals that promote neointima formation, in concert with additional determinants, that is, the protooncogene Bcl-xL and the neomatrix constituent tenascin, which were recently shown to be involved in neointima formation (3,21).

No evidence for transmigration of adventitial cells. Our quantitative, compartment-specific data do not show significant changes in medial cellularity reflecting transmigration of cells from adventitia to neointima between days 4 and 28 after angioplasty, while formation of hyperplastic neointima and hypercellular adventitial remodeling occur (Fig. 1). In addition, Bcl-2 signaling in the media was sparse, and constitutive HSP47 expression remained unchanged (Fig. 5B). If it is true that Bcl-2 and HSP47 act as survival factors for neointimal and adventitial cells, medial expression should be increased in case of transmural migration. Also, the inner adventitial layer was characterized by sparse cellularity (Fig. 6). Particularly in this corridor, we detected neither HSP47 nor Bcl-2 signaling, although parallel expression of both determinants was maximal in the outer adventitia and the innermost neointima (Figs. 5 and 6). Likewise, in traumatized rat carotid arteries whose adventitial cells were subsequently treated with PKH26 fluorescin stain, no labeled cells were detected in the media at days 3 and 5 or in the neointima at day 14 (31). Taken together, these data in rats do not give evidence for transmural migration of adventitial cells, and indirectly support intimal and/or circulating progenitor cells as source of neointima.

Of note, data from an animal restenosis model cannot directly be extrapolated to the clinical scenario in patients. Among several drawbacks, the factors mediating the vascular response to injury in humans are not identical to those in rodents. Animal models usually lack the high-grade preexisting atherosclerotic lesions with its complex architecture. Also, it should be noted that quan-

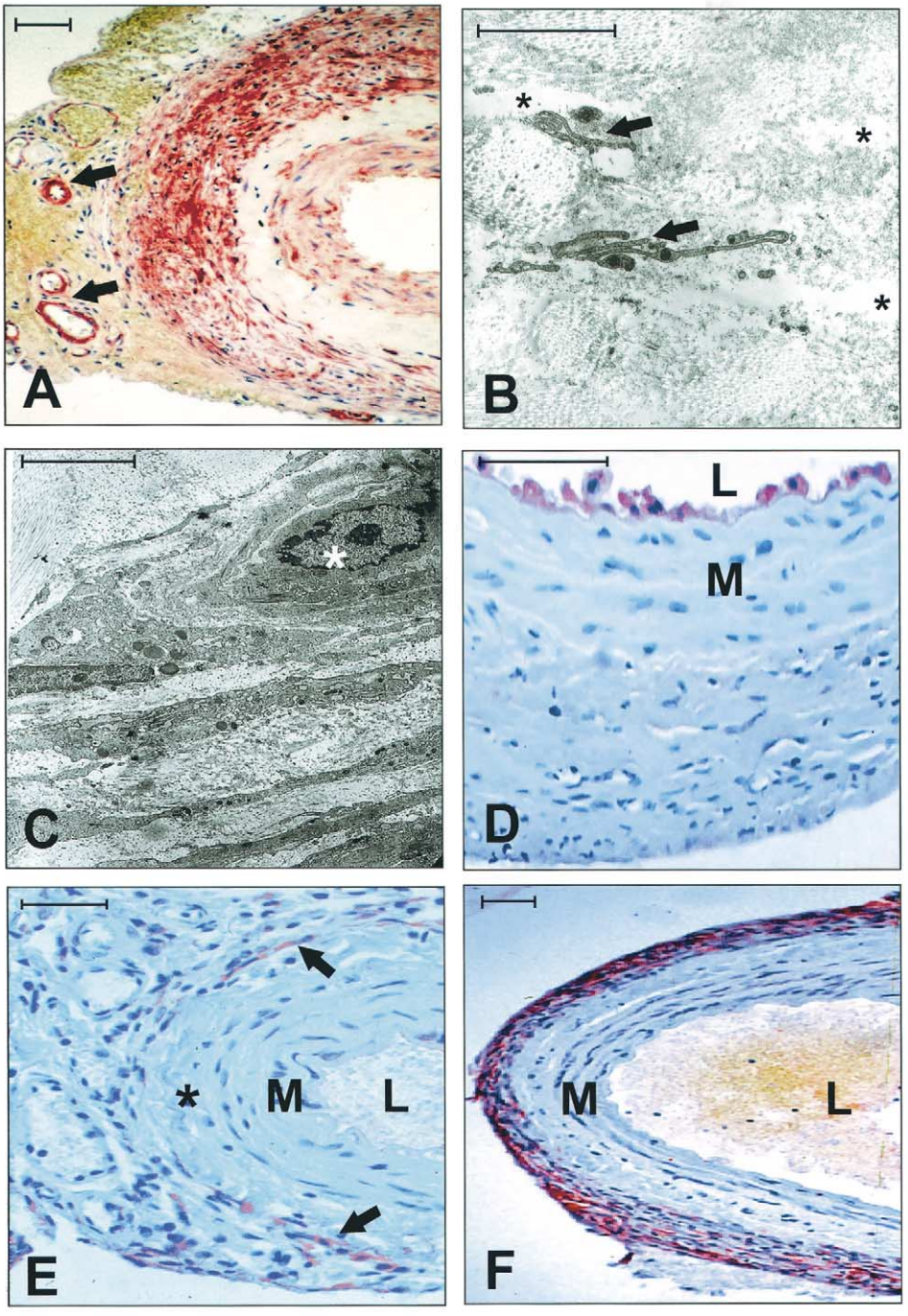

Figure 6. Photomicrographs of transmural response to injury, focused on adventitial remodeling. **(A)** Intense α-smooth muscle actin immunoreactivity in the media and outer adventitia at day 4; also perivascular microvessels of the vasa vasorum are positive **(arrows)**. **(B)** Transmission electron microscopy detail of hypocellular inner adventitia at day 7 illustrating two cells that simultaneously display end-stage apoptotic shrinkage **(arrows)**; see large regions of non-structured matrix **(*)**. **(C)** Transmission electron microscopy detail of hypercellular outer adventitia at day 7 showing several viable cells with fibroblast-like appearance embedded in dense extracellular matrix. Also, see in the endothelial cell lining a perivascular capillary **(*)**. **(D)** No signals of OX-62$^+$ dendritic cells are found in the media (M) and the broad adventitia at day 4, in contrast to intense OX-62 immuno-staining along the luminal surface. **(E)** Cell-bound B-cell lymphoma 2 protein signals are exclusively found in the outer adventitia **(arrows)** at day 4. While demarcation from perivascular connective tissue is not always possible, inner adventitia **(*)**, M, and lumen (L) can be easily distinguished. **(F)** Transmural heat shock protein 47 expression pattern at day 4. Note the distinct immuno-staining exclusively located in the outer adventitia. **Bar** = 50 μm **(A, D to F)**; **bar** = 5 μm **(B, C)**.

titative immunohistochemistry is a technique fraught with potential artifactual influences including sampling error, section thickness, staining variability, dilutions, and blocking, etc. Whenever possible, these limitations were overcome by a large number of analyzed probes and controls within animal experimentation and tissue staining procedures.

Taken together, in perspective to potential clinical implications, the present data of neointimal Bcl-2$^+$HSP47$^+$ DC accumulation highlight these determinants as potential candidates for a specific local modulation at the injured vasculature, for example, by drug-eluting stents. In particular, DCs, which exclusively populate the neointimal site, seem to be attractive as carriers for targeted therapies such as DC-mediated gene transfer.

Reprint requests and correspondence: Dr. Gerhard Bauriedel, Department of Cardiology, University of Bonn, Sigmund-Freud-Str. 25, D-53105, Bonn, Germany. E-mail: Gerhard.Bauriedel@ukb.uni-bonn.de.

REFERENCES

1. Clowes AW, Reidy MA, Clowes MM. Kinetics of cellular proliferation after arterial injury. Lab Invest 1983;49:327–33.
2. Li G, Chen SJ, Oparil S, Chen YF, Thompson JA. Direct in vivo evidence demonstrating neointimal migration of adventitial fibroblasts after balloon injury of rat carotid arteries. Circulation 2000;101:1362–5.
3. Wallner K, Sharifi BG, Shah PK, Noguchi S, DeLeon H, Wilcox JN. Adventitial remodeling after angioplasty is associated with expression of tenascin mRNA by adventitial myofibroblasts. J Am Coll Cardiol 2001;37:655–61.
4. Christen T, Verin V, Bochaton-Piallat ML, et al. Mechanisms of neointima formation and remodeling in the porcine coronary artery. Circulation 2001;103:882–8.
5. Sata M, Saiura A, Kunisato A, et al. Hematopoietic stem cells differentiate into vascular cells that participate in the pathogenesis of atherosclerosis. Nat Med 2002;8:403–9.
6. Han CL, Campbell GR, Campbell JH. Circulating bone marrow cells can contribute to neointimal formation. J Vasc Res 2001;38:113–9.
7. Kalka C, Masuda H, Takahashi T, et al. Transplantation of ex vivo expanded endothelial progenitor cells for therapeutic neovascularization. Proc Natl Acad Sci USA 2000;97:3422–7.
8. Gill M, Dias S, Hattori K, et al. Vascular trauma induces rapid but transient mobilization of VEGFR2+AC133+ endothelial precursor cells. Circ Res 2001;88:167–74.
9. Saiura A, Sata M, Hirata Y, Nagai R, Makuuchi M. Circulating smooth muscle progenitor cells contribute to atherosclerosis. Nat Med 2001;7:382–3.
10. Simper D, Stalboerger PG, Panetta CJ, Wang S, Caplice NM. Smooth muscle progenitor cells in human blood. Circulation 2002;106:1199–204.
11. Banchereau J, Briere F, Caux C, et al. Immunobiology of dendritic cells. Annu Rev Immunol 2000;18:767–811.
12. Caux C, Vanbervliet B, Massacrier C, et al. CD34+ hematopoietic progenitors from human cord blood differentiate along two independent dendritic cell pathways in response to GM-CSF+TNFα. J Exp Med 1996;184:695–706.
13. Hansson GK, Libby P, Schönbeck U, Yan ZQ. Innate and adaptive immunity in the pathogenesis of atherosclerosis. Circ Res 2002;91:281–91.
14. Bobryshev YV, Lord RSA. Mapping of vascular dendritic cells in atherosclerotic arteries suggests their involvement in local immune-inflammatory reactions. Cardiovasc Res 1998;37:799–810.
15. Ozmen J, Bobryshev YV, Lord RSA, Ashwell KWS. Identification of dendritic cells in aortic atherosclerotic lesions in rats with diet-induced hypercholesterolemia. Histol Histopathol 2002;17:223–37.
16. Wick G, Romen M, Amberger A, et al. Atherosclerosis, autoimmunity, and vascular-associated lymphoid tissue. FASEB J 1997;11:1199–207.
17. Millonig G, Niederegger H, Rabl W, et al. Network of vascular-associated dendritic cells in intima of healthy young individuals. Arterioscler Thromb Vasc Biol 2001;21:503–8.
18. Brenan M, Puklavec M. The MRC OX-62 antigen: a useful marker in the purification of rat veiled cells with the biochemical properties of an integrin. J Exp Med 1992;175:1457–65.
19. Bennett MR, Evan GI, Schwartz SM. Apoptosis of rat vascular smooth muscle cells is regulated by p53-dependent and -independent pathways. Circ Res 1995;77:266–73.
20. Bauriedel G, Schluckebier S, Hutter R, et al. Apoptosis in restenosis versus stable-angina atherosclerosis—implications for the pathogenesis of restenosis. Arterioscler Thromb Vasc Biol 1998;18:1132–9.
21. Pollman MJ, Hall JL, Mann MJ, Zhang L, Gibbons GH. Inhibition of neointimal cell bcl-x expression induces apoptosis and regression of vascular disease. Nat Med 1998;4:222–7.
22. Ryan JJ, Prochownik E, Gottlieb CA, et al. C-myc and bcl-2 modulate p53 function by altering p53 subcellular trafficking during the cell cycle. Proc Natl Acad Sci USA 1994;91:5878–82.
23. Nopora A, Brocker T. Bcl-2 controls dendritic cell longevity in vivo. J Immunol 2002;169:3006–14.
24. Nagai N, Hosokawa M, Itohara S, et al. Embryonic lethality of molecular chaperone Hsp47 knockout mice is associated with defects in collagen biosynthesis. J Cell Biol 2000;150:1499–505.
25. Rocnik E, Chow LH, Pickering JG. Heat shock protein 47 is expressed in fibrous regions of human atheroma and is regulated by growth factors and oxidized low-density lipoprotein. Circulation 2000;101:1229–33.
26. Andrié R, Skowasch D, Lentini S, Dinkelbach S, Lüderitz B, Bauriedel G. Human heat shock proteins 47 and 60 as determinants of plaque instability in human coronary atheroma (abstr). Eur Heart J 2001;22 Suppl:294.
27. Bauriedel G, Hutter R, Welsch U, Bach R, Sievert H, Lüderitz B. Role of smooth muscle cell death in advanced coronary primary lesions: implications for plaque instability. Cardiovasc Res 1999;41:480–8.
28. Bauriedel G, Kandolf R, Schluckebier S, Welsch U. Ultrastructural characteristics of human atherectomy tissue from coronary and lower extremity arterial stenoses. Am J Cardiol 1996;77:468–74.
29. Mosse PR, Campbell GR, Wang ZL, Campbell JH. Smooth muscle phenotypic expression in human carotid arteries: comparison of cells from diffuse intimal thickenings adjacent to atheromatous plaques with those of the media. Lab Invest 1985;53:556–62.
30. Weiss L. The blood. In: Weiss L, editor. Cell and Tissue Biology. Baltimore, MD: Urban & Schwarzenberg, 1988:425–43.
31. DeLeon H, Ollerenshaw JD, Griendling KK, Wilcox JN. Adventitial cells do not contribute to neointimal mass after balloon angioplasty of the rat common carotid artery. Circulation 2001;104:1591–3.
32. Aicher A, Heeschen C, Mohaupt M, et al. Nicotine strongly activates dendritic cell-mediated adaptive immunity: potential role for progression of atherosclerotic lesions. Circulation 2003;107:604–11.
33. Okamoto E, Couse T, DeLeon H, et al. Perivascular inflammation after balloon angioplasty of porcine coronary arteries. Circulation 2001;104:2228–35.
34. Cremer I, Dieu-Nosjean MC, Maréchal S, et al. Long-lived immature dendritic cells mediated by TRANCE-RANK interaction. Blood 2002;100:3646–55.
35. Durand E, Mallat Z, Addad F, et al. Time courses of apoptosis and cell proliferation and their relationship to arterial remodeling and restenosis after angioplasty in an atherosclerotic rabbit model. J Am Coll Cardiol 2002;39:1680–5.
36. Frisch SM, Ruoslahti E. Integrins and anoikis. Curr Opin Cell Biol 1997;9:701–6.